Available online at www.sciencedirect.com

ScienceDirect

Energy Procedia 69 (2015) 913 – 924

Energy Procedia

International Conference on Concentrating Solar Power and Chemical Energy Systems, SolarPACES 2014

Investigation of cascaded shell and tube latent heat storage systems for solar tower power plants

M. Liu[a,]*, N.H.S Tay[a], M. Belusko[a] and F. Bruno[a]

[a]*Barbara Hardy Institute, University of South Australia, Mawson Lakes Boulevard, Mawson Lakes, SA5095, Australia*

Abstract

Solar thermal electricity generation is taking up increasing proportions of future power generation worldwide. Recent research indicates that a closed-loop Brayton cycle using supercritical carbon dioxide (s-CO_2) offers the potential of higher power cycle efficiency versus the conventional superheated steam cycle at temperatures relevant for CSP applications. Thermal energy storage solves the time mismatch between the solar energy supply and the electricity peak demand and allows for a more efficient use of the turbine and other power block components. The narrow storage temperature range required for the s-CO_2 cycle advantages the use of latent heat storage, which has a higher storage density compared to the conventional two-tank storage. This paper demonstrates a design of a cascaded shell and tube phase change storage system potentially applicable for the s-CO_2 cycle. A previously developed effectiveness-number of transfer unit method is employed as a design guide and computational fluid dynamics modelling is performed to examine the sensible energy extraction. The results prove that the effectiveness of the extracted sensible energy can be increased by increasing the number of phase change storage systems in series. Stainless steel (SS) AISI 316 as well as a creep resistant SS AISI 446 is considered as the tube material in the design and results suggest that using AISI 446 can minimize the overall amount of storage and tube materials.

Peer review by the scientific conference committee of SolarPACES 2014 under responsibility of PSE AG

Keywords: Thermal storage; Phase change material; CSP; Supercritical carbon dioxide power cycle.

* Corresponding author. Tel.: +61 8 8302 5132; fax: +61 8 8302 3380.
E-mail address: ming.liu@unisa.edu.au

Peer review by the scientific conference committee of SolarPACES 2014 under responsibility of PSE AG
doi:10.1016/j.egypro.2015.03.175

1. Introduction

Using concentrating solar power (CSP) technology to generate electricity is of great interest internationally. The most common power cycle currently employed by existing CSP plants is Rankine cycle using subcritical steam. The turbine efficiency is limited to 42% with a maximum operating temperature of around 655 °C, which is the practical limit for the steel alloy turbine materials [1]. Brayton power cycle using supercritical carbon dioxide (s-CO_2) has been proposed and investigated by a few groups [2-4] and thermodynamic cycle analysis indicated that the s-CO_2 cycle allows for a potential higher efficiency compared to steam Rankine cycles at dry cooling conditions [4].

Thermal energy storage technology allows improved dispatch-ability of power output from the CSP plant and increases the plant's annual capacity factor. Most existing thermal energy storage systems currently use two-tank sensible heat storage with molten salts at 290 °C (cold tank) and 565 °C (hot tank). Latent heat storage using phase change materials (PCMs) potentially allows a large amount of energy to be stored in a relatively small volume by using the material's heat of fusion, resulting in a smaller and less costly storage system compared to sensible thermal storage systems. A significant amount of the energy is also stored and released at a constant temperature.

The cascaded latent heat storage is a promising solution as it offers a higher utilization of the possible phase change and a more uniform heat transfer fluid outlet temperature compared with the single PCM storage system [5]. Michels and Pitz-Paal [6] experimentally studied a vertical shell and tube heat storage system with $NaNO_3$ and three PCMs (KNO_3, KNO_3/KCl and $NaNO_3$) connected in series, respectively. The results showed that the single PCM was completely molten at the end of the charging but only 2% of the material was solidified in the discharging, which means 98% of energy was lost. In the three-PCM system, 92% of the PCM was molten at the end of charging and around 67% was solidified at the end of discharging. Farid and Kanzawa [7] and Farid et al. [8] evaluated the thermal performance of a thermal storage system employing three PCMs and proved that there is around 10% increase in the heat transfer rate during both the charging and discharging processes versus the system with one PCM. In a packed bed thermal storage system with five PCMs, the efficiency is improved by 13-26% compared to a single PCM system [9]. Furthermore, the second-law analysis has been carried out by multiple groups [10-12] and the results suggested that the second-law efficiency can be improved significantly by employing more than one PCM.

The effectiveness is a significant performance parameter to evaluate the actual energy exchanged within the PCM thermal storage system. Tay et al. [13] developed the effectiveness-number of transfer units (ε-NTU) method and experimentally validated it for refrigeration applications where the amount of sensible energy is negligible. This method has been developed for various PCM storage configurations [14-16] and has a distinct advantage in design. It enables the designer to determine the actual heat transfer rate for a specific fraction of the PCM. Consequently, the amount of the material and the specifications of the heat transfer area can be quickly determined.

This paper presents a design of a cascaded latent heat storage system, which enables a discharge duration of 6 hours for a 50 MWh solar tower power plant using s-CO_2 as the heat transfer medium. The analysis was conducted for a shell and tube type storage system with the PCM located between the tubes. This arrangement has been recognized as the most promising configuration for a latent heat storage system requiring high efficiency with a minimum volume [17]. The design parameters of the storage system, such as the number, length and diameter of the tubes, are estimated by using the ε-NTU method. Three-dimensional computational fluid dynamics (CFD) modelling by using ANSYS (version 15.0) was conducted to analyse the transient heat transfer behavior during charging and discharging.

Nomenclature

A	Heat transfer area (m^2)
CF	compact factor
C_p	specific heat of the HTF (kJ/(kg K))
E	energy storage density (kWhr/kg)
ε	instantaneous effectiveness

δ	PCM liquid fraction
R_T	total thermal resistance (K/W)
R_{HTF}	thermal resistance of the HTF (K/W)
R_{WALL}	thermal resistance of the tube wall (K/W)
R_{PCM}	thermal resistance of the PCM (K/W)
R_i	inner radius of the tube (m)
R_o	outer radius of the tube (m)
L	length of the tube (m)
h_f	heat transfer coefficient of the HTF (W/(m^{2}K))
kw	thermal conductivity of the tube wall (W/(mK))
k_{PCM}	thermal conductivity of the PCM (W/(mK))
T_{in}	HTF inlet temperature (°C)
T_{out}	HTF outlet temperature (°C)
T_{PCM}	PCM melting temperature (°C)
TF	total storage fraction
U	heat transfer coefficient (W/(m^{2}K))
Q_{HTF}	energy delivered by the heat transfer fluid (kW)
Q_{latent}	latent energy stored in the PCM (kW)
$Q_{sensible}$	sensible energy stored in the PCM (kW)
$\dot{m}$	HTF mass flow rate (kg/s)
M_{PCM}	amount of PCM required (tons)
$M_{PCM,\ ideal}$	ideal amount of PCM required (tons)
M_{final}	final amount of PCM required (tons)

2. Design parameters

A PCM thermal storage system was designed and applicable to a simple recuperative s-CO_2 Brayton power cycle configuration. The design of the PCM storage system is based on indirect storage, in which the thermal energy is indirectly stored in the PCM with s-CO_2 (20 MPa) as the working fluid in both the solar field and the power block. The advantages of this arrangement are the operational hazards and costs associated with solidification of molten salt are avoided. Also, the heat exchanger between the power block and the thermal system is removed. The use of s-CO_2 rather than molten salts as the heat transfer fluid leads to a reduction in the heat transfer performance of the storage system. However, as identified by Liu et al. [18], the heat transfer fluid has a limited impact on the heat exchange rate due to the high heat transfer area required in the indirect PCM storage system. The storage system is a horizontal shell and tube (tube-in-tank) design, in which the high pressure s-CO_2 flows through the tube contained in the shell of the storage vessel (Fig. 1).

As per the description for a simple s-CO_2 Brayton cycle in [2, 4], the specifications for the storage system are presented in Table 1. Compared to the conventional molten salt power towers with steam turbines, the useful temperature differential for storage is less. This lower temperature differential advantages the use of PCM, where the latent component of storage is more dominant.

Table 1. Specifications for storage system.

Charging inlet temperature	600 °C
Discharging inlet temperature	375 °C
Required turbine inlet temperature	550 °C
Working fluid pressure	20 MPa
Thermal capacity of the storage system	120 MW

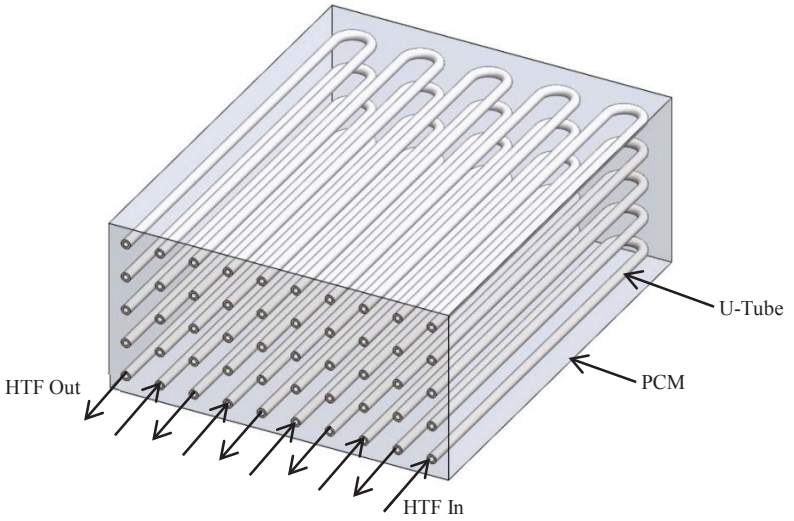

Fig. 1. Tube-in-tank (shell and tube) PCM energy storage system with U-Tube.

The design of the coil was based on stainless steel (SS) AISI 316 and AISI 446. At temperatures of 550 °C and above, given the high internal pressure within the tube, for SS316, the failure due to creep is the critical design criterion. AISI 316 is being considered on the basis that it has reasonable corrosion resistance to the selected PCMs and also is due to its low cost. AISI 446 is considered due to its ability to operate at high temperature and resistant to creep. The corrosion resistance of this material has not been investigated. Based on a designers' handbook [19], for a 100,000 hour life at 600 °C, the stress to achieve rupture is 25 MPa. Based on this matching the hoop stress, together with a safety factor of 2.5, the tube design was fixed at inner diameter of 12 mm and a wall thickness of 5 mm for AISI 316 and 1 mm for AISI 446. This range was considered as the maximum range of material being considered. Further analysis is needed on these criteria, and is beyond the scope of this study.

A PCM system with three different PCMs was investigated in this study. A schematic diagram of a solar tower power plant with a cascaded PCM storage system is presented in Fig. 2. To achieve a suitable storage system for CSP applications, the highest melting point of the PCM must match the required turbine inlet temperature. The PCM selected is a eutectic mixture of sodium carbonate, potassium carbonate and lithium carbonate ($Na_2CO_3/K_2CO_3/Li_2CO_3$) with a melting temperature of 550 °C [20]. A nominal latent heat of fusion of 200 kJ/kg was chosen to represent the average value across a range of salt mixtures [20]. To investigate the value of multiple PCMs, the second and the third PCMs were given the same properties, as indicated in Table 2. The chosen melting point for the second (492 °C) and the third PCM (433 °C) was based on an equal temperature difference between each PCM during discharging.

Table 2. Thermo-physical properties for three PCMs.

Latent heat of fusion (*kJ/kg*)	Specific heat (*J/(kg·K)*)	Thermal conductivity (*W/(m·K)*)		Density (kg/m^3)
		Solid	Liquid	
200	1500	0.5	1.83	2000

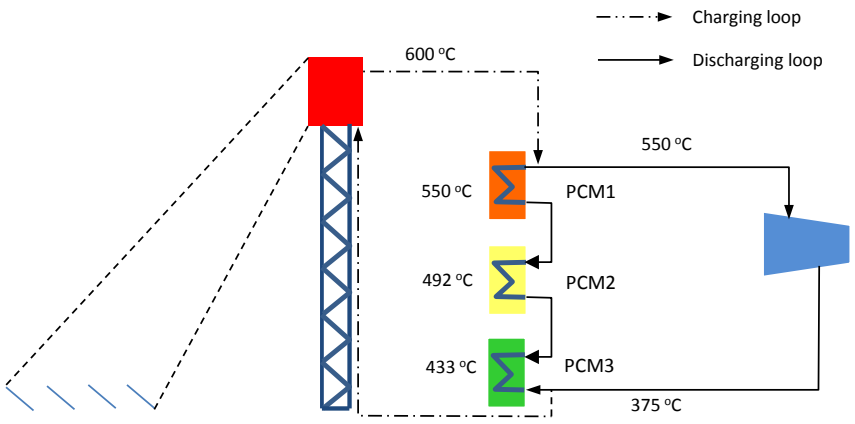

Fig. 2. Schematic diagram of a solar tower power plant with a cascade PCM storage system.

The energy storage density of the storage material determines the size and the cost of the storage system. Based on the PCM properties, the total energy storage density of the material, *E*, over a temperature range from 375 to 550 °C is 0.128 kW·h/kg, considering both the latent and the sensible energy. However, for indirect PCM storage systems, the actual storage density is defined by the PCM volumetric fraction and the effectiveness in both charging and discharging, as investigated by Tay et al. [21]. Eq. 1 presents the useful energy storage density which can directly be compared to sensible storage.

$$E_{useful} = CF \cdot \varepsilon_{charge} \cdot \varepsilon_{discharge} \cdot E \tag{1}$$

With regards to applying this method to the CSP case, the effectiveness for charging and discharging are defined by Eqs. 2 and 3.

$$\varepsilon_{charge} = {(T_{in} - T_{out})}\Big/{(T_{in} - T_{PCM})} \qquad \text{where } T_{in} \text{ is 600 °C} \tag{2}$$

$$\varepsilon_{discharge} = {(T_{in} - T_{out})}\Big/{(T_{in} - T_{PCM})} \qquad \text{where } T_{in} \text{ is 375 °C} \tag{3}$$

Previous research involved experimentally investigating the average effectiveness of a tube-in-tank arrangement within the PCM demonstrating its relationship to the average NTU (Eq. 4) [22, 23]. This average effectiveness can be derived from the local effectiveness, through evaluating the local thermal resistance between the heat transfer fluid and the PCM at the phase change front, in terms of the phase change fraction (Eq. 4). The average NTU represents the 1D average thermal resistance to heat transfer between the HTF and the PCM at the phase change front (Eq. 5). The thermal resistance is defined by the resistance in the convection layer of the fluid, and the conduction layer of the tube wall and PCM component which has already undergone phase change (Eq. 6) as shown in Fig. 3.

$$\bar{\varepsilon} = \int_0^1 \varepsilon_\delta \cdot d\delta = 1 - e^{-\overline{NTU}} \tag{4}$$

The average NTU can be presented by:

$$\overline{NTU} = (\overline{\mathrm{UA}})/(\dot{m}C_p) = 1/(\overline{R_T}\dot{m}C_p) \tag{5}$$

$$\overline{R_T} = \int_0^1 R_T = \int_0^1 \left\{ {1}\Big/{\left(2\pi \mathrm{R_i} L h_f\right)} + {\left(\ln\left({R_o}/{R_i}\right)\right)}\Big/{\left(2\pi \mathrm{k_w} L\right)} + {\left(\ln\left\{\frac{\left[\left\{\delta\left(\mathrm{R_{max}}^2 - \mathrm{R_o}^2\right) + \mathrm{R_o}^2\right\}^{1/2}\right]}{\mathrm{R_o}}\right\}\right)}\Big/{\left(2\pi L k_{PCM}\right)} \right\} \tag{6}$$

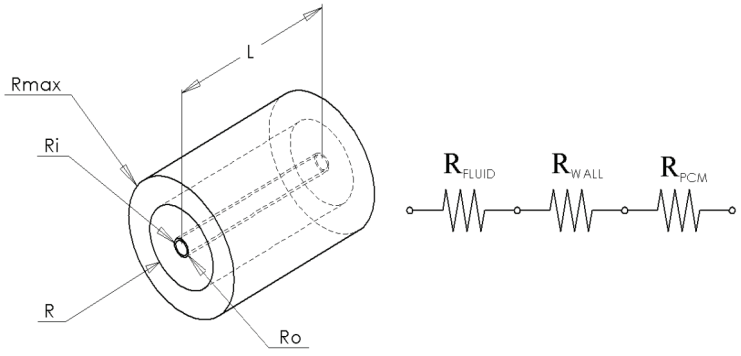

Fig. 3. Simplified model of the round shape factor (a) and thermal circuit (b) [13].

The ε-NTU method has been well developed for refrigeration applications where the amount of sensible energy is negligible. Sensible energy storage is a significant component in CSP applications and in this case it represents 57% of the total energy density. However, given that an improved effectiveness for heat transfer during phase change will also translate to the improved effectiveness for heat transfer in sensible heat, it can be argued that the method can be particularly helpful as a tool for comparing designs. Final design will be achieved through the use of CFD. In this case, the design can be evaluated, by determining the effectiveness as a function of the total storage fraction (Eq. 7).

$$\boldsymbol{TF} = {\boldsymbol{Q_{HTF}}}\Big/{\left(\boldsymbol{Q_{latent}} + \boldsymbol{Q_{sensible}}\right)} \tag{7}$$

3. CFD modeling

3.1. Model description

Three-dimensional CFD modelling using ANSYS code which has been validated experimentally [15, 24] was used to analyse the transient heat transfer during the phase change process of different configurations of PCM arrangements as shown in Fig. 4 and Table 3, subject to either charging or discharging. A number of simulations were conducted for the charging and discharging processes. Details of the simulations conducted can be found in Table 4. The modelling of the phase change thermal energy storage system was based on the unsteady Navier-Stokes equations. The continuity, momentum, and energy equations follow the CFD model developed by Tay et al. [15, 24].

Table 3. Parameters of the configurations of PCM arrangements.

	W (m)	Length (m)	Width (m)	Height (m)	Ri (m)	Ro (m)
Single PCM (SS316)	0.08027	1	0.1605	0.0827	0.006	0.011
Multiple PCMs (SS446)	0.08027	0.333	0.1605	0.0827	0.006	0.011
Multiple PCMs (SS446)	0.0392	0.333	0.0784	0.0392	0.006	0.007

Similar to previous work [15, 24], the CFX-PRE of the academic research code ANSYS was utilised. Three domains were created; the HTF and PCM were created as fluid domains while the tubes were created as a solid domain. The HTF and tube domains used the hexahedral cells while tetrahedral cells were assigned to the PCM domain. The grid dependency of the model was created based on the validated models developed by Tay et al. [15, 24]. Liquid and solid PCMs were created separately and added into a homogeneous binary mixture with a saturation temperature set as the phase change temperature. A sub-domain was also added to the PCM domain to create a large sink term. The convergence criterion of 1E-04 was applied. The time step for both the charging and discharging processes were set to 10 s. All boundary and initial conditions were similar to the model developed by Tay et al. [24].

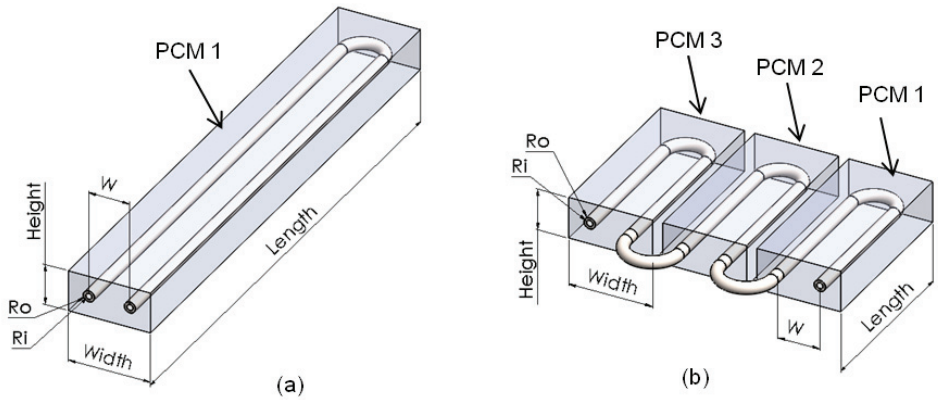

Fig. 4. Details of simplified tube-in-tank model for (a) single PCM and (b) multiple PCMs.

Table 4. Parameters of the simulations conducted in ANSYS.

		Processes	HTF $\dot{m}$ (kg/s)	HTF Inlet Temp. (°C)	PCM Initial Temp. (°C)	W (m)
Case a	Single PCM (SS316)	Charging	0.005	600	545	0.0827
Case b	Single PCM (SS316)	Charging	0.005	600	375	0.0827
Case c	Single PCM (SS316)	Discharging	0.0005	375	555	0.0827
Case d	Multiple PCMs (SS316)	Discharging	0.0005	375	555	0.0827
Case e	Multiple PCMs (SS446)	Discharging	0.0005	375	555	0.0392

3.2. E-NTU validation

To demonstrate the validity of the ε-NTU at identifying the actual heat transfer rate, a CFD analysis was conducted for the charging (case a) where there is small sensible energy component within the PCM. Using the ε-NTU analysis, the mass flow rate selected for the tube was 0.005 kg/s and the effectiveness was a function of the liquid phase change fraction as presented in Fig. 5. In this case, the majority of the thermal resistance to heat transfer occurs in the PCM. Taking the outlet temperature and the specified liquid fraction from the CFD analysis, the local

effectiveness as a function of the liquid fraction could be determined, and is presented in Fig. 5. Generally a good agreement is shown, with the ε-NTU mostly understating the effectiveness. After a liquid phase change fraction of 0.95, the effectiveness begins to drop dramatically, deviating from the ε-NTU.

Fig. 6 shows the liquid phase change fraction (LF) during charging at different stages of the phase change process, at different sections of the U tube. The figure shows that on average the thickness of the liquid fraction layer along the tube is constant at every time step. This is best reflected at the 900 mm from the inlet section, which is the mid-point of the U tube. This shows assuming 1D heat flow in the ε-NTU method adequately represents the average phase boundary during the phase change. At the 5 hour point, there was no longer any frozen PCM remaining around almost half the tube. This reflects a loss of heat exchange area between the tube and the PCM at the phase change front. At this point the effectiveness dramatically drops. Overall, the ε-NTU adequately determines the heat transfer from 95% of the stored energy during charging where the sensible component is negligible. Therefore, the ε-NTU can be used as a comparative design guide for this type of latent storage system.

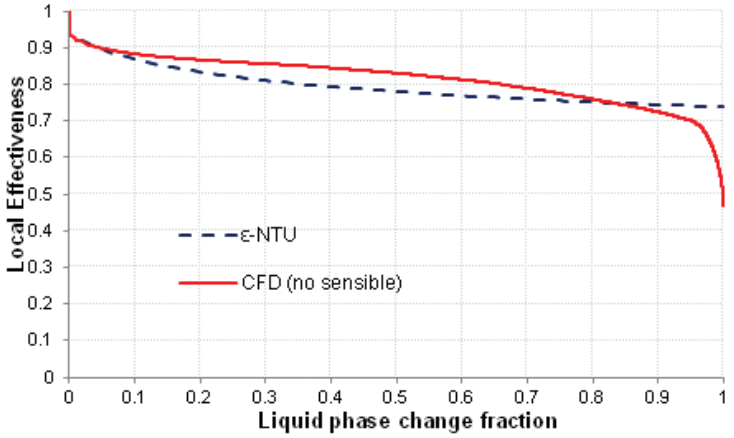

Fig. 5. Comparison of the local effectiveness during charging of PCM 1 with AISI 316.

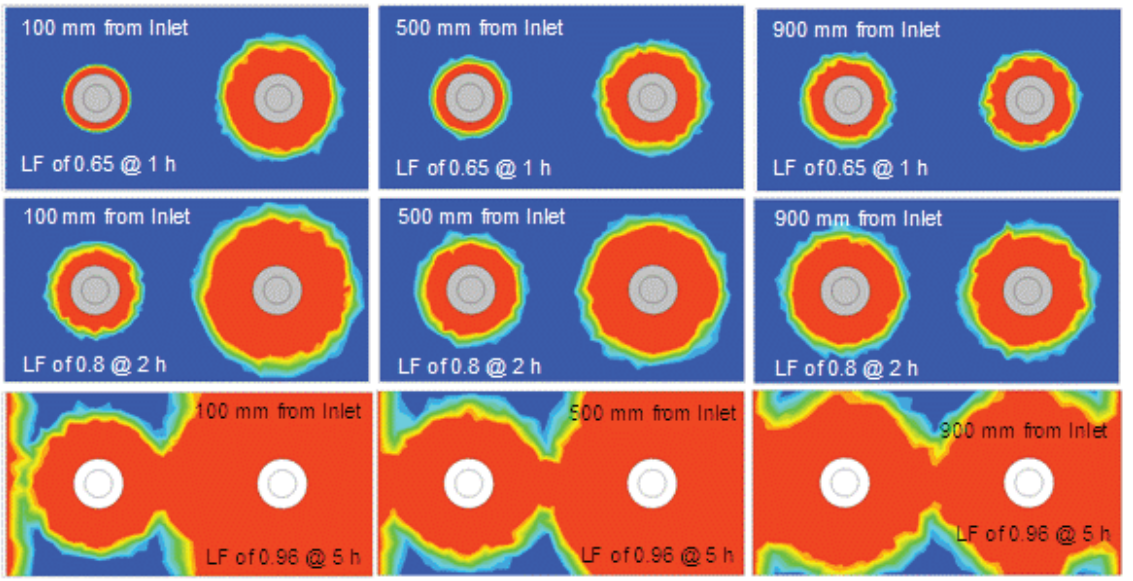

Fig. 6. Cross-section for a single PCM system at different liquid phase change fractions and time.

3.3. Multiple PCMs

During discharging, the resistance to the heat transfer within the PCM is defined by the thermal conductivity of the solid PCM. Given that the solid PCM's thermal conductivity is much lower than the liquid PCM, the focus of the thermal performance will be on discharging, as charging is expected to have a higher effectiveness.

To investigate the impact of multiple PCMs, a CFD model was conducted on a single U tube with PCM 1 (case c), and three PCMs (case d) applying the same PCM volume and tube length (Fig. 4(b)). Using the ε-NTU, a mass flow rate of 0.0005 kg/s was determined. Fig. 7 shows the effectiveness as a function of the total storage fraction which includes both the sensible and latent storage energy. It was found that during discharging; the latent energy is transferred first followed by the sensible component. The first observation shown in Fig. 7 is that during the phase change, the multiple PCM experiences a lower effectiveness. This can be explained by each PCM having 1/3 of the area to transfer heat for the same mass flow rate, and therefore resulting in a higher thermal resistance. Of more significance, this result shows that extracting useful sensible energy stored within the PCM from a single PCM is limited, with the effectiveness dropping dramatically after the end of phase change. This drop occurs as the heat transfer fluid is unable to exchange heat with a high temperature source, as the U tube arrangement generally delivers a uniform temperature distribution. Multiple PCMs can potentially alleviate this problem by separating the temperature within the sensible storage. The sensible energy is distributed within the PCM 1 at lowest temperature and the PCM 3 at the highest temperature. Therefore the heat transfer fluid is able to exchange heat with a high temperature source. For an effectiveness of 0.8, 55% of the total storage fraction is useful for the multiple PCM case while for a single PCM this value is only 45%. Therefore, increasing the number of tanks in series enables greater extraction of the stored sensible energy.

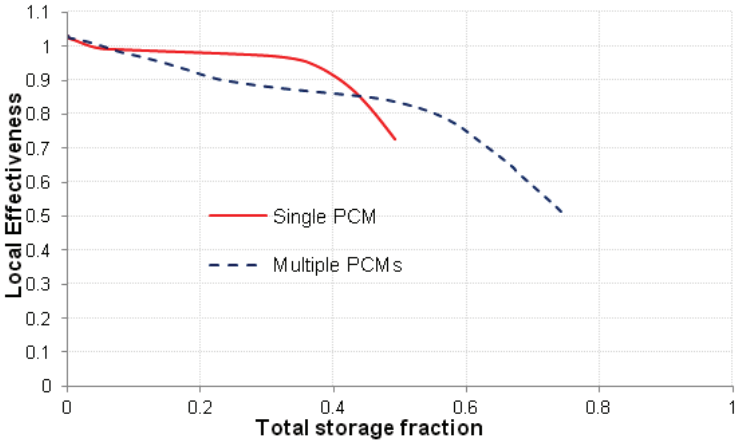

Fig. 7. Comparison of single to multiple PCMs with AISI 316 design.

4. Design of PCM storage systems

Using the ε-NTU as a design guide, the geometry and tube material was determined, after which CFD was used to investigate the number of tanks in series to maximise the extraction of the sensible energy. The amount of PCM is defined by the load requirements and factors related to the expected useful energy that can be stored within the system. The amount of each PCM was determined based on nominal values from which the effectiveness was determined. Using this effectiveness the final size of the system could be found, and the amount of PCM was adjusted accordingly. Ultimately, any design process is techno-economic. Therefore, consideration of the amount of the tube material relative to PCM was a design requirement.

4.1. E-NTU design

The PCM storage system is taken to be an array of tanks, where for each PCM, a number of tanks are in parallel and each group of tanks for each PCM are in series. For each tank, a diameter of 4 m was applied, and the tube velocity was limited to 20 m/s, consistent with steam boilers. This was achieved by increasing the number of PCM tanks in parallel for each PCM. It was found that the thermal resistance in the heat transfer fluid, had a negligible impact on the NTU, and therefore the number of tanks in parallel was fixed at 15. Consequently, in the design process, any adjustment in the mass flow rate in each tube had a corresponding adjustment in the tube length and as per Eq. 5, resulted in no change in the NTU. Fluid properties of s-CO_2 were determined based on the average of the inlet and outlet temperatures across the PCM system. Based on the maximum discharge thermal output over the ideal temperature range of 375 to 550 °C, the mass flow rate of 560 kg/s was determined. The amount of PCM was determined based on the ideal thermal load of 720 MWh, and for simplicity, the mass of each PCM was equal.

Beginning the design process at PCM 3, based on a chosen volume fraction of the PCM, the average effectiveness could be found. Then the average outlet temperature could be identified which became the inlet temperature for PCM 2. Following the same process the final average outlet temperature from PCM 1 could be determined, after which the overall average heat exchange effectiveness was determined. The same process was applied to charging, from which the overall charging effectiveness could be found. In this case, the mass flow rate was determined based on the ideal temperature change from 600 °C to the melting point of PCM 3, and found to be 588 kg/s.

The design parameter used was the volume fraction of the PCM, as this directly relates to the amount of PCM and tube material. This parameter determined the volume of PCM around each tube which ultimately defines the thermal resistance in the PCM. This figure was adjusted to balance the amount of stainless steel tube compared to the mass of PCM, on a cost basis and the effectiveness. It was estimated that at approximately 20% of the PCM mass, the cost of the tube and PCM per volume of tank were similar. Overall for AISI 316, a volume fraction of 0.94 was chosen resulting in the mass of tube equating to 17% of the PCM mass. This resulted in a tube spacing of 80 mm. The design process was repeated using AISI 446. In this case, the volume fraction was limited to 0.9 and the mass of tube is equal to 11% of the PCM mass. The tube spacing reduced to 39 mm.

Table 5 presents the average effectiveness for charging and discharging for each design. From this effectiveness, the final size of the PCM system can be identified based on the ε-NTU. This analysis does not consider the effectiveness in extracting sensible energy stored, and should only be used comparatively. As explained in Tay et al. [21], the effectiveness is also a measurement of the actual energy exchanged divided by the total maximum energy exchanged. Therefore the mass of PCM that will enable 720 MWh of delivered energy to be extracted from the thermal storage is defined by Eq. 8. Consequently, the amount of PCM and tube materials needed with AISI 316 is 8,703 and 1,479 tons, respectively, and with AISI 446 is 5,777 and 635 tons, respectively. These values translate to AISI 316 requiring 50% more PCM and 2.3 times more tube material than by using AISI 446. This clearly demonstrates that using creep resistant tube material is able to minimise the amount of tube material and maximise the thermal performance and hence to minimise the system size and the cost.

$$M_{PCM} = M_{PCM,ideal}/(\varepsilon_{charge} \cdot \varepsilon_{discharge}) \quad (8)$$

Table 5. Average effectiveness for charging and discharging for AISI316 and AISI446.

	AISI 316		AISI 446	
	Charging	Discharging	Charging	Discharging
PCM 1	0.81	0.49	0.99	0.93
PCM 2	0.81	0.49	0.99	0.92
PCM 3	0.81	0.49	0.99	0.92
System	0.92	0.70	1.00	0.97

4.2. CFD design

To consider the system performance in extracting sensible energy storage, CFD modelling of the design was conducted. From the ε-NTU, the design with AISI 446 has a tube length for each PCM at 5.6 m, giving a total tube length of 16.8 m with a flow rate of 0.0046 kg/s. If the tube length is reduced to 2 m, this gives a mass flow rate of 0.005 kg/s. Fig. 8 presents the effectiveness as a function of the total fraction for this design. It shows that approximately half the total fraction is useful. From Fig. 8, it was found that at the total fraction of 0.54, the effectiveness is 0.8. Beyond this point, the effectiveness of the system decrease dramatically. Taking the charging effectiveness to be unity, the final mass of the PCM was found to be 14,353 tons based on Eq. 9.

$$M_{Final} = M_{PCM,ideal}/TF/\varepsilon_{discharge}/\varepsilon_{charge} \quad (9)$$

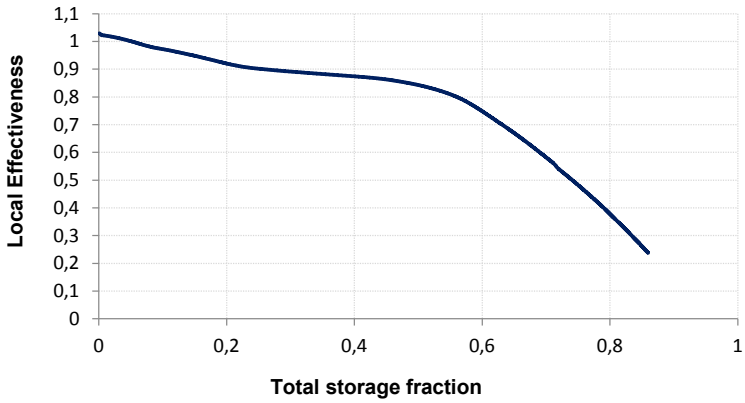

Fig. 8. Comparison of local effectiveness during discharging for multiple PCMs with AISI 446 design.

5. Conclusions

A design process has been undertaken on a tube-in-tank PCM storage system that is potentially suitable for the s-CO_2 Brayton cycle, using the ε-NTU method and CFD modelling. Using the CFD, the ε-NTU method was found to adequately determine the local effectiveness for energy transfer of the latent phase in the U Tube design. Therefore, the ε-NTU method is effective as a comparative design tool. The CFD modelling identified that, a multiple PCM arrangement is required to effectively extract sensible energy stored within the PCM. Using the ε-NTU method, designs were developed considering both AISI 316 and 446. It was demonstrated that maximising the material strength could minimise the overall amount of PCM and tube materials. Increasing the number of PCM systems in series increases the effectiveness of the extracted sensible energy storage. Therefore, a number of useful strategies to achieve an effective design have been demonstrated which will enable an optimised design to be developed. However, designing a cascaded PCM storage system for an actual CSP plant is quite complex and this paper only presents some preliminary work and more detailed study will be carried out in the future work.

Acknowledgements

The authors Liu, Tay and Belusko are funded through individual fellowships provided by the Australian Government, through the Australian Renewable Energy Agency (ARENA). This research was performed as part of the Australian Solar Thermal Research Initiative (ASTRI), a project supported by the Australian Government, through ARENA.

References

[1] Renac Renewable Academy. ReGrid: Concentrated Solar Power. 2013.
[2] Dostal V, Driscoll MJ, Hejzlar P. A supercritical carbon dioxide cycle for next generation nuclear reactors. Massachusetts Institute of Technology, 2004 MIT-ANP-TR-100.
[3] Neises TW, Turchi C. A comparison of supercritical carbon dioxide power cycle configurations with an emphasis on CSP applications SolarPACES 2013; 2013; Las Vegas, USA: Elsevier Ltd.
[4] Turchi CS, Ma Z, Neises TW, Wagner MJ. Thermodynamic Study of Advanced Supercritical Carbon Dioxide Power Cycles for Concentrating Solar Power Systems. Journal of Solar Energy Engineering 2013;135(4):041007.
[5] Michels H, Hahne E. Cascaded latent heat storage for solar thermal power stations. EuroSun'96; 1996; Freiburg, German.
[6] Michels H, Pitz-Paal R. Cascaded latent heat storage for parabolic trough solar power plants. Solar Energy 2007;81(6):829-37.
[7] Farid MM, Kanzawa A. Thermal performance of a heat storage module using PCM's with different melting temperatures: mathematical modeling. Journal of Solar Energy Engineering 1989;111(2):152-7.
[8] Farid MM, Kim Y, Kansawa A. Thermal performance of a heat storage module using PCM's with different melting temperature: experimental. Journal of Solar Energy Engineering 1990;112(2):125-31.
[9] Adebiyi GA, Hodge BK, Steele WG, Jalalzadeh-Azar A, Nsofor EC. Computer simulation of a high-temperature thermal energy storage system employing multiple families of phase-change storage materials. Journal of Energy Resources Technology 1996;118(2):102-11.
[10] Aceves-Saborio S, Nakamura H, Reistad GM. Optimum efficiencies and phase change temperatures in latent heat storage systems. Journal of Energy Resources Technology 1994;116(1):79-86.
[11] Domanski R, Fellah G. Exergy analysis for the evaluation of a thermal storage system employing PCMS with different melting temperatures. Applied Thermal Engineering 1996;16(11):907-19.
[12] Li Y-Q, He Y-L, Wang Z-F, Xu C, Wang W. Exergy analysis of two phase change materials storage system for solar thermal power with finite-time thermodynamics. Renewable Energy 2012;39(1):447-54.
[13] Tay NHS, Belusko M, Bruno F. An effectiveness-NTU technique for characterising tube-in-tank phase change thermal energy storage systems. Applied Energy 2012;91(1):309-19.
[14] Belusko M, Halawa E, Bruno F. Characterising PCM thermal storage systems using the effectiveness-NTU approach. International Journal of Heat and Mass Transfer 2012;55(13–14):3359-65.
[15] Tay NHS, Bruno F, Belusko M. Experimental validation of a CFD and an e-NTU model for a large tube-in-tank PCM system. International Journal of Heat and Mass Transfer 2012;55:5931-40.
[16] Amin NAM, Belusko M, Bruno F, Liu M. Optimising PCM thermal storage systems for maximum energy storage effectiveness. Solar Energy 2012;86(9):2263-72.
[17] Erek A, Ilken Z, Acar MA. Experimental and numerical investigation of thermal energy storage with a finned tube. International Journal of Energy Research 2005;29(4):283-301.
[18] Liu M, Belusko M, Steven Tay NH, Bruno F. Impact of the heat transfer fluid in a flat plate phase change thermal storage unit for concentrated solar tower plants. Solar Energy 2014;101:220-31.
[19] Tay NHS., Belusko M, and Bruno F, Experimental investigation of tubes in a phase change thermal energy storage system. Applied Energy 2012; 90(1):288-97.
[20] American Iron and Steel Institute. High temperature characteristics of stainless steel - A designers' Handbook Series No.9004: Nickel Development Institute. Available from: www.nickelinstitute.org.
[21] Kenisarin MM. High-temperature phase change materials for thermal energy storage. Renewable and Sustainable Energy Reviews 2010;14(3):955-70.
[22] Tay NHS, Belusko M, Bruno F. Designing a PCM storage system using the effectiveness-number of transfer units method in low energy cooling of buildings. Energy and Buildings 2012;50:234-42.
[23] Castell A, Belusko M, Bruno F, Cabeza LF. Maximisation of heat transfer in a coil in tank PCM cold storage system. Applied Energy 2011;88(11):4120-7.
[24] Tay NHS, Belusko M, Bruno F. Experimental investigation of tubes in a phase change thermal energy storage system. Applied Energy 2012;90(1):288-97.